

## **Quantifying the variability in interpretation of shear testing of a natural fracture.**

Franco, M.A., Potter, J., Ross, B.J.

*Geotechnical Center of Excellence, The University of Arizona, Tucson, Arizona, USA*

Copyright 2023 ARMA, American Rock Mechanics Association

This paper was prepared for presentation at the 57<sup>th</sup> US Rock Mechanics/Geomechanics Symposium held in Atlanta, Georgia, USA, 25-28 June 2023. This paper was selected for presentation at the symposium by an ARMA Technical Program Committee based on a technical and critical review of the paper by a minimum of two technical reviewers. The material, as presented, does not necessarily reflect any position of ARMA, its officers, or members. Electronic reproduction, distribution, or storage of any part of this paper for commercial purposes without the written consent of ARMA is prohibited. Permission to reproduce in print is restricted to an abstract of not more than 200 words; illustrations may not be copied. The abstract must contain conspicuous acknowledgement of where and by whom the paper was presented.

**ABSTRACT:** The shear strength of discontinuities (e.g., joints, bedding planes, faults) plays an important role in the mechanical behavior of a rock mass and is crucial to the analysis and design of rock slopes. The shear strength of natural discontinuities is typically determined by performing a series of direct shear tests. Several sources of variability in direct shear test results are recognized by the geotechnical community (e.g., the inherent variability of shear strength in a rock mass, joint roughness), but the effect of variations in testing equipment, testing methods, and in the interpretation and application of test results has been little studied. The focus of this paper is the potential variance introduced by the interpretation of direct shear test results. The authors explore potential variation in a single direct shear test by examining test results from a natural joint with four different approaches. Potential future research paths are also discussed.

### 1. BACKGROUND

The direct shear test (DST) is widely used to determine the shear strength of natural discontinuities in rock and soil. This determination is of particular importance when designing rock-based engineering structures and assessing failures. Direct shear tests are performed using a shear box apparatus that maintains a constant force normal to the discontinuity while applying an increasing shear force parallel to the discontinuity (ASTM, 2016). The information recorded includes the applied normal force, displacement of the top of the specimen in relation to the bottom, the shear force applied to achieve that displacement, and fracture roughness. The test is generally performed three to four times with increasing applied normal loads, resulting in a set of traces corresponding to the applied normal forces. Figure 1 illustrates an idealized trace resulting from a direct shear test. Recorded forces are then converted to stresses by dividing by the surface contact area measured at the time of the test.

Two parameters are calculated based on the trace data described above (ASTM, 2016):

- **Peak shear strength** is associated with the maximum shear stress value along a sheared surface attained during a test.
- **Residual shear strength** is associated with the point at which the shear stress remains essentially constant with increasing shear displacement.

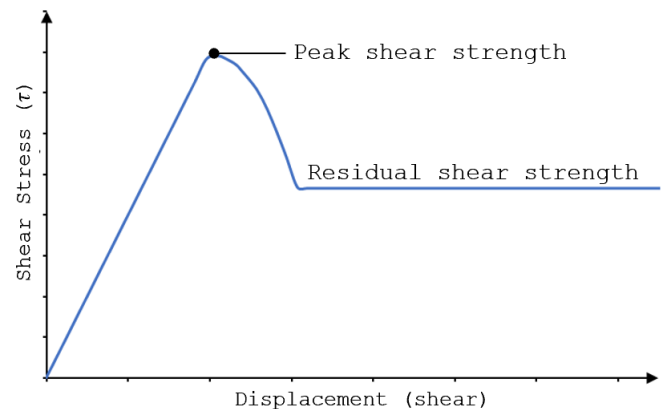


*Fig 1. Idealized shear stress versus shear displacement trace, with points defining peak and residual shear strength identified. Modified from ASTM, 2016.*

Once a shear strength value has been chosen from each of the traces that compound the test, these are matched to the

corresponding normal stresses and depicted in a shear stress versus normal stress plane as shown in Figure 2.

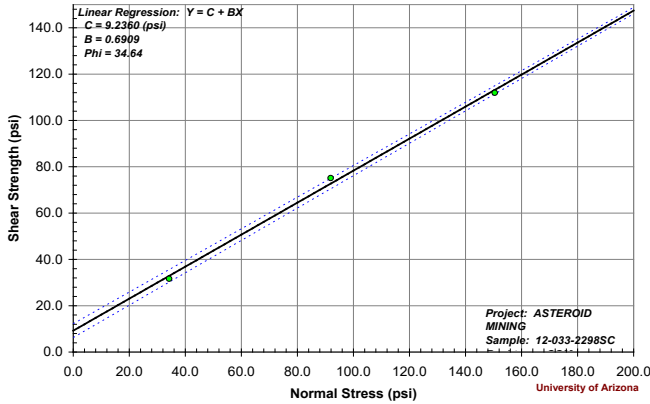


Fig 2. Example direct shear test results shown in the shear stress versus normal stress plane (University of Arizona).

The peak shear strength for a sample can generally be determined from the maximum shear stress value attained. In contrast, the determination of the residual shear strength can be a complicated and subjective process in cases where the behavior of the post-peak section of the trace is fluctuating. The post-peak region is defined here as the full section of the shear stress-displacement curve after the peak shear stress has been reached. Figure 1 shows an idealized schematic in which the post-peak trace levels out at a consistent shear stress value. This is an idealized case in which the residual point can be easily determined from the definition of residual shear strength defined above. Figure 3 shows the dataset used in this study for which the post-peak region is variable and the selection of a residual shear stress value is more challenging and potentially dependent on practitioner judgment. The fact that the interpretation of datasets is the product of the expertise and judgment of designers represents a potential source of variability in direct shear testing.

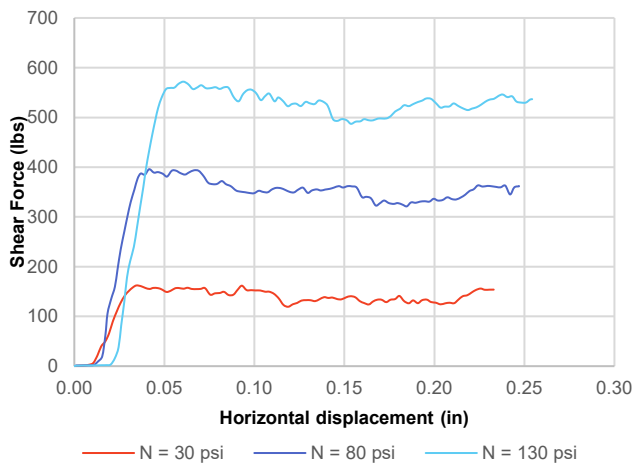


Fig 3. Direct shear traces for open quartz monzonite fracture (study sample obtained from University of Arizona Rock Mechanics Laboratory).

A number of suggested methods and standards, including Gyenge and Herget (1977), Hencher and Richards (1989), and Muralha et.al. (2014), discuss the calculation of shear strength parameters from both the peak shear stress and residual shear stress. However, methodologies for determining residual shear strength are not described in detail for cases in which the behavior of the post-peak section of a trace is fluctuating.

The aim of this paper is to quantify the variability that shear strength parameters might exhibit when different approaches to the selection of residual shear stresses are implemented. To do this, the authors used methodologies to quantify variability in potential residual shear strength selections.

An undisturbed, 25.4 mm (1 in) high and 67.8 mm (2.67 in) diameter drill core natural fracture sample specimen was collected from a mine in Northern Arizona. The sample lithology is quartz monzonite with visible quartz, feldspar, biotite, and hornblende and has a medium-grained texture with an average grain size of 2.5 millimeters. The color of the sample is light gray with yellowish tones.

The test was carried out three times under increasing normal forces of 743.3, 1988.4, and 3233.9 N (168, 447, and 727 lbf) at a rate of 0.635 mm/min (0.025 in/min). An HM-2560A shear device manufactured by Humboldt Machinery, which can apply a normal force up to 2000 lbs was used. The sample was sheared through a natural joint with a 3612.9 mm<sup>2</sup> (5.6 in<sup>2</sup>) area. The sample was reversed back to the starting point prior to the start of each test.

The rock sample described above, the test details, and the testing machine specifications were provided by the University of Arizona rock mechanics laboratory. This paper is a data analysis work and the authors have not participated in the testing process.

No tilt correction, which accounts for the direction and amount of sample tilt, was applied to the study data. Photos of the top and bottom surfaces of the sample are shown in Figure 4.

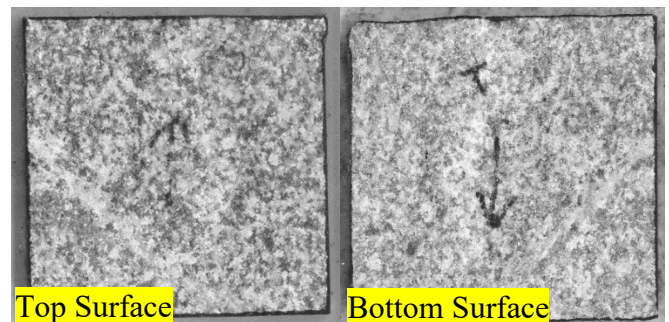


Fig 4. Photos of the quartz monzonite open fracture tested for this study.

## 2. METHODOLOGY

The following is a description of the four approaches proposed in this study to select residual shear stress values from the post-peak region of the traces in the dataset. Shear stress values were selected for each trace and paired with the appropriate normal stress. This “selection-pairing” process resulted in a total of three shear stress versus normal stress couples (Figure 2). A linear regression was then performed through the three points or ‘couples’ (Figure 2). Friction angle and cohesion were then calculated using the Mohr-Coulomb criterion, where shear strength ( $\tau$ ) is equal to cohesion ( $c$ ) plus the normal force ( $\sigma$ ) times the tangent of the friction angle ( $\phi$ ), as shown in Eq. (1). (Terzaghi et al., 1996).

$$\tau = c + \sigma \tan\phi \quad (1)$$

The decision to use the selected criterion for estimating the shear strength of the joint used for this study is based on the method’s simplicity, the authors’ familiarity with it, and its popularity in the field as highlighted by Singh et al. (2011).

The process of selecting shear stresses for each trace and coupling them with appropriate normal stresses is referred to here as a combination. The number of combinations varies depending on the approach employed. The number of combinations determines the number of shear strength parameters (friction angle and cohesion) calculated for a given method. For this study, linear values determined using the Mohr-Coulomb criteria (cohesion and frictional angle) are used to quantify shear strength. The authors acknowledge that a power curve would be more representative of the shear strength of an open fracture, but linear values are used for descriptive purposes.

### 2.1. Peak, Average, Minimum Approach (1)

As its name implies, this approach compares shear strength parameters calculated from the peak, average, and minimum shear stress values for all post-peak points on Traces A, B, and C. Figure 5 illustrates the location of the selected points on each trace for this method. The red stars and dashed line correspond to the peak, the orange dots and dashed line to the average, and the green dots and dashed line to the minimum shear stresses. Their values and the resulting friction angles are also displayed. Table 1 summarizes cohesion and friction angle values calculated from the Peak-Average-Minimum Approach residual point selections.

This is the only approach where the peak shear stress is included in the selection. This approach was selected to determine how well the maximum, minimum, and average peak and post-peak values can provide a general description of the data set as a whole.

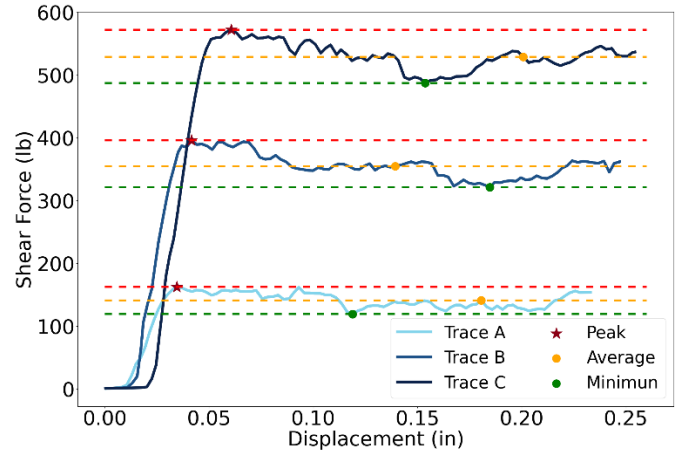


Fig 5. Illustration of the Peak, Average, Minimum Approach

Table 1. Peak-Ave-Min Approach Summary Statistics

	Cohesion (psi)	Friction Angle (deg)
Count	3	3
Mean	6.03	34.77
St. Dev.	3.06	1.44
Min	3.00	33.33
1 <sup>st</sup> Quartile	4.48	34.05
Median	5.97	34.77
3 <sup>rd</sup> Quartile	7.55	35.50
Max	9.12	36.22

### 2.2. Displacement Approach (2)

This approach consists of breaking the traces out into increments of 0.127 mm (0.005 in) displacements and calculating the associated shear strength at each increment. Shear strength parameters were calculated from the three trace points associated with displacement values starting at 1.905 mm (0.075 in) and increasing at a sample interval of 0.127 mm (0.005 in) (Figure 6). For instance, after three minutes of testing, the displacement equaled 1.905 mm (0.075 in). as highlighted by the first dashed line on the left. The dashed red lines shown in Figure 6 show the Displacement selection intervals. To cover the post-peak region of the A, B, and C traces, thirty sets of shear strength parameters were calculated between 1.905 mm (0.075 in). and 5.715 mm (0.225 in). Table 2 summarizes cohesion and friction angle values calculated from the Displacement Approach residual point selections.

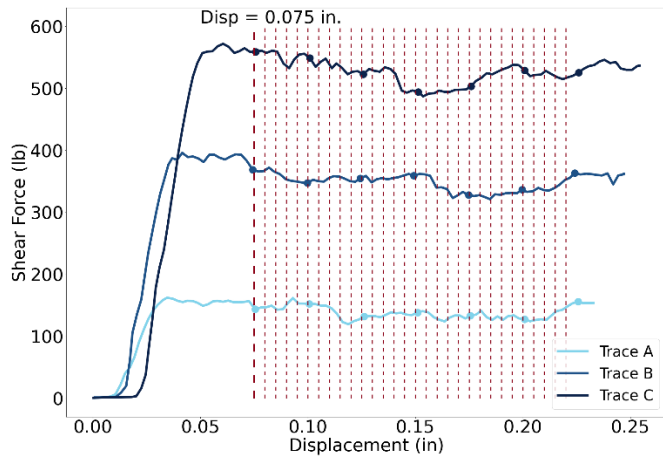


Fig 6. Illustration of the Displacement Approach

Table 2. Displacement Approach Summary Statistics

	Cohesion (psi)	Friction Angle (deg)
Count	30	30
Mean	4.98	34.79
St. Dev.	2.35	1.25
Min	1.11	32.39
1 <sup>st</sup> Quartile	2.92	33.68
Median	5.31	35.14
3 <sup>rd</sup> Quartile	6.26	35.69
Max	9.32	36.72

### 2.3. Differentiation Approach (3)

This strategy is based on the authors' analysis of the sample's trace behavior. It was assumed for the purposes of this study that increases in shear force in the post-peak region of the trace are associated with asperities. When an asperity impedes the displacement of the bottom part of the specimen during testing, the shear force must be increased until the asperity is surpassed or sheared off. The authors propose that these observed asperities can be correlated between traces based on increases in shear force along each trace. To identify these points, an operation denominated differentiation is performed. This operation consists of selecting a specific point on the trace and subtracting the value of the preceding point from the selected point's value. The sign of value resulting from this calculation indicates whether the previous shear stress value is larger or smaller than the selected value. If the sign is positive, the previous value is smaller indicating a positive slope. Conversely, if the sign of the result is negative, the slope between the preceding and selected points is negative. For this approach, all points that were immediately preceded by a positive slope and immediately followed by a negative slope were

selected and considered potential asperities. Figure 7 presents several examples of what are assumed to be asperities identified along each trace. The dashed red lines represent the shear stress combinations that were obtained. Table 3 summarizes cohesion and friction angle values calculated from the Differentiation Approach residual point selections.

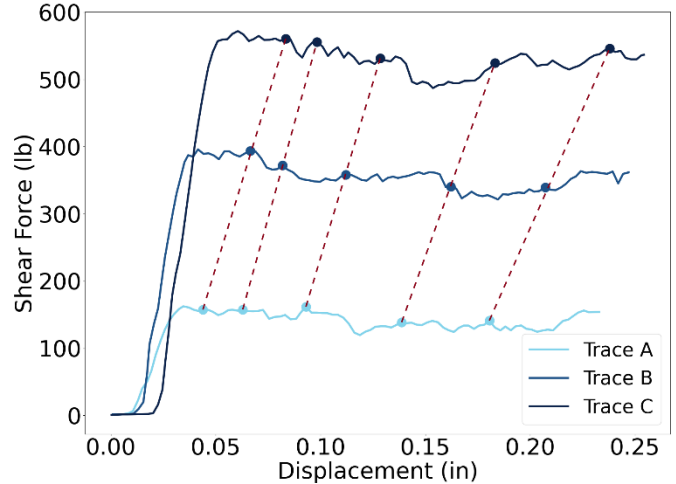


Fig 7. Illustration of the Differentiation Approach. Dashed red lines connect points that the author has assumed are associated with the same asperity.

Table 3. Differentiation Approach Summary Statistics

	Cohesion (psi)	Friction Angle (deg)
Count	5	5
Mean	8.66	34.28
St. Dev.	2.25	1.82
Min	5.48	31.66
1 <sup>st</sup> Quartile	7.78	33.29
Median	8.43	34.66
3 <sup>rd</sup> Quartile	10.78	35.79
Max	10.84	36.00

### 2.4. Permutations Approach (4)

This approach was selected to quantify and evaluate all possible combinations and related shear stress calculations. This was done by iteratively selecting a point from each of the three traces and calculating the associated shear strength for each three-point combination. This resulted in a total of 517,920 combinations of three post-peak points from which a shear strength could be calculated. A single combination is referred to here as a permutation. As an example, if we refer to the first point after the peak from Trace A as Point A-1 and the next point moving right along the x-axis as Point A-2, the first permutation considered included Point A-1, Point B-1 (first post-peak point on Trace B), and Point C-1 (first post-peak point on Trace C). The second permutation considered included Point A-1, Point B-2,

and Point C-1. This logic was repeated until all possible combinations in the dataset were defined. This approach provided a range of friction angle and cohesion values that represent all possible residual shear strength values a practitioner could possibly select.

Five permutations were randomly chosen from the larger dataset and are presented in Figure 8. Points having the same color represent values of the same combination. Table 4 summarizes cohesion and friction angle values calculated from the Permutations Approach residual point selections.

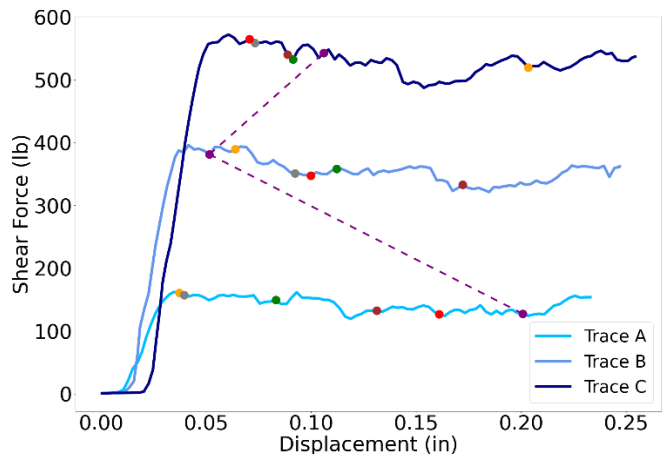


Fig 8. Illustration of the Permutations Approach. Five permutations (from a total of 517,000) are shown here as an example.

	Cohesion (psi)	Friction Angle (deg)
Count	517920	517920
Mean	6.17	34.72
St. Dev.	3.26	1.55
Min	-4.17	30.25
1 <sup>st</sup> Quartile	3.78	33.67
Median	6.21	34.82
3 <sup>rd</sup> Quartile	8.50	35.79
Max	16.59	38.83

### 3. RESULTS

Summary statistics of friction angle and cohesion calculated from each of the four approaches are provided in Tables 5 and 6 for comparison. The friction angle ranged between approximately 30 degrees and 43 degrees, and the cohesion ranged between approximately -4.2 and 16.5 psi across all methods. Note that some combinations considered for the Permutations Approach resulted in negative cohesion. All combinations are presented here for comparison. However, it should be noted that, in practice, if negative cohesions are observed,

the testing and/or interpretation procedures should be reevaluated.

The Permutations Approach (4) had the highest range in values. However, between the other three approaches, fewer number of combinations did not necessarily mean a smaller range in variability. For the Differentiation Approach (3), five combinations were evaluated, and the difference is smaller than the Peak, Average, and Minimum Approach (1) which consisted of only three combinations. This is to be expected given that the Peak, Average, Minimum Approach considers the extreme values from each trace. Figures 9 and 10 present the same data in the form of Box and Whisker plots.

Approach	Points Sampled	Friction Angle (deg)		
		Max	Min	Difference
1	3	36.22°	33.33°	2.89°
2	30	36.72°	32.39°	4.33°
3	5	36.00°	31.66°	4.34°
4	517920	38.83°	30.25°	8.58°

Approach	Points Sampled	Cohesion (psi)		
		Max	Min	Difference
1	3	9.12	2.99	6.13
2	30	9.32	1.11	8.21
3	5	10.84	5.48	5.36
4	517920	16.59	-4.17	20.59

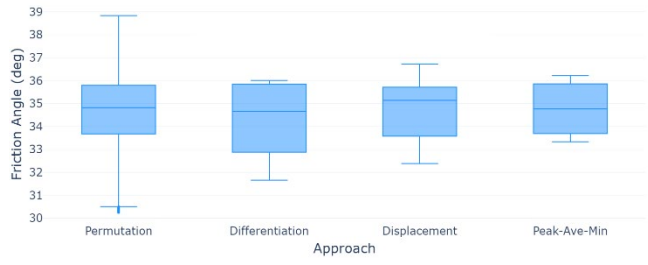


Fig 9. Box and Whisker plot of calculated friction angles for all approaches.

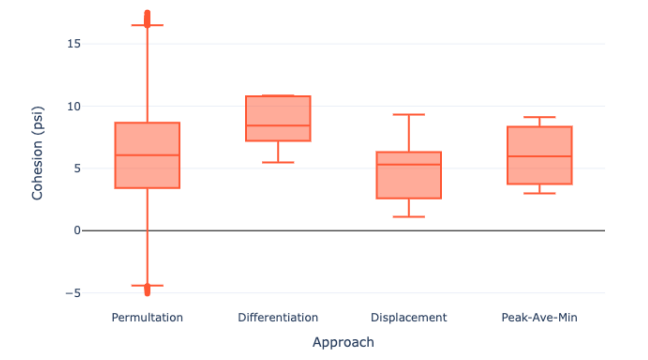


Fig 10. Box and whisker plot of calculated cohesion for all approaches.

The data was also evaluated in terms of shear strength ( $\tau$ ), which was calculated for each combination at 60 psi and 120 psi normal stress, as shown in Figure 11. Note that when comparing the approaches, the Displacement Approach provides the lowest mean shear strength at both normals considered for the sample studied here. The Differentiation Approach results in the highest mean shear strength at both normals considered, likely due to the fact that the approach considers local maximums, and therefore higher shear stresses were selected for each trace.



Fig 11. Box and Whisker plots of shear strength ( $\tau$ ) calculated at 60 psi normal (above) and 120 psi normal (below) stresses.

Figures 12 and 13 show the same data presented in Figure 11 as distributions of shear strength ( $\tau$ ) at 60 and 120 psi normal for the approach with the most combinations and highest range in values (Permutations Approach). Table 7 presents the distribution of shear strength for the Permutations Approach at five-percentile intervals. For this approach, shear strength varied between approximately 42.5 and 52.9 psi (10.4 psi difference) at a 60-psi normal stress and 82.1 and 96.4 psi (14.3 psi difference) at a 120-psi normal stress. This indicates that, when considering all possible combinations, the shear strength could vary by as much as 15 to 20 percent.

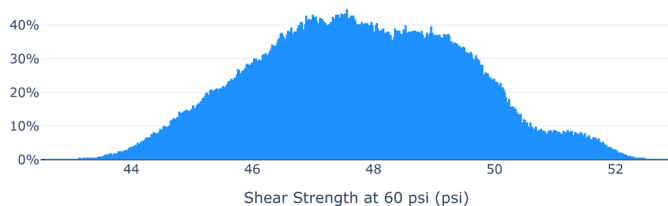


Fig 12. Distribution of shear strength ( $\tau$ ) at 60 psi normal for permutations approach

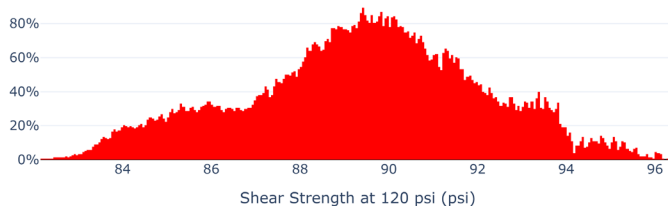


Fig 13. Distribution of shear strength ( $\tau$ ) at 120 psi normal for permutations approach

Table 7. Distribution of Shear Strength at 60psi and 120psi Normal for Permutations Approach

Percentile	Tau at 60psi	Tau at 120 psi
0%	42.52	82.16
5%	44.95	84.66
10%	45.49	85.58
15%	45.90	86.38
20%	46.24	87.17
25%	46.53	87.74
30%	46.80	88.20
35%	47.04	88.57
40%	47.28	88.91
45%	47.52	89.23
50%	47.76	89.53
55%	48.01	89.83
60%	48.27	90.14
65%	48.53	90.46
70%	48.80	90.81
75%	49.07	91.23
80%	49.34	91.65
85%	49.65	92.19
90%	50.03	92.91
95%	50.68	93.67
100%	52.93	96.42

#### 4. OBSERVATIONS AND CONCLUSIONS

The following are observations and conclusions determined from this study:

- i. Within the standards and suggested methods reviewed by the authors, a definition is provided for residual shear stress or its equivalent. It refers to the shear stress value that remains constant while shear displacement continues. However, there is a notable absence of detailed discussion on how to identify or select this residual shear stress when the behavior of the residual portion of the stress-displacement curve is not steady and several fluctuations are perceived. This research paper has demonstrated that there are hundreds of thousands of possibilities

in which shear stresses could be combined from a single trace to calculate residual shear strength from a direct shear test. The presence of such a vast array of options represents a variability originated from human observations that is not measured or accounted for in current practices. Consequently, there is a need for further investigation and development of standardized approaches to address this variability.

- ii. When considering the repeatability of the approaches presented, it is likely that the Peak-Average-Minimum (1) and Displacement (2) Approaches to analyzing potential variability in residual values would be most applicable on a production scale. The Differentiation (3) Approach requires significant user input and judgment prior to the calculation of strength parameters. This indicates the approach itself is subjective and may not be the best measure of sample variability. It also resulted in higher mean shear strength values, indicating it is the least conservative approach. The Permutations (4) Approach provides more results than what could reasonably be considered by a practitioner, however, with the aid of a computer program to calculate and combine or select appropriate residual strengths, it does prove useful in evaluating the total range of possible residual values.
- iii. There may be a case when the bottom part of a sample hits an asperity and cannot shear it. As a consequence, the sample could lift. This means that the applied normal force is no longer perpendicular to the discontinuity. These points should not be considered in the analysis because the condition of maintaining a fixed normal force is not met. As the authors did not perform the test, it is not definitively known which points should be discarded and the resulting ranges might vary.

## 5. FUTURE WORK

- i. Future work to assess the variability introduced by practitioner methodology will include increasing the data set by repeating this analysis on a series of samples of varying complexity. Once a larger data set has been analyzed, the findings support the larger study described in the preceding point.
- ii. The impact of roughness, stiffness, and dilation were not considered in this study. Future work is needed to determine the effect of these parameters on the approaches presented here.
- iii. It is known that the stress behavior of a rock discontinuity is anisotropic, non-linear, and depends on the state of stresses (Nassir et. Al,

2013). Since many applications demand knowledge of the behavior of rocks under generalized stress conditions, future work may include repeating this study considering either Power Law or Barton-Bandis shear strength criterion.

## ACKNOWLEDGEMENTS

We would like to thank Dave Nicholas, Christian Obregon, Julian Venter, Edward Wellman, and Ian Stilwell for their guidance and support throughout the research process. We would also like to thank David Streeter at the University of Arizona for his assistance with the data.

The work presented here is in support of an initiative originated at the Geotechnical Center of Excellence at the University of Arizona to evaluate variability in the interpretation of direct shear tests. The overall project goals are intended to summarize the current state of direct shear testing, establish best practices for determining the residual shear strength of natural fractures, and develop a tool to facilitate decision-making for geotechnical designers.

## REFERENCES

1. ASTM. (2016). Standard Test Method for Performing Laboratory Direct Shear Strength Tests of Rock Specimens Under Constant Normal Force.
2. Gyenge, M. and G. Herget. (1977). Determination of strength properties of rock discontinuities by direct shear test. *Pit slope manual supplement 3-2: Laboratory tests for design parameters*, Canmet report 77-26: 37-44.
3. Hencher, S.R., and L.R. Richards. (1989). Laboratory direct shear testing of rock discontinuities. *Ground Engineering*, 22, 2: 24-31.
4. Singh, M., Raj A. and Singh B. (2011). Modified Mohr–Coulomb criterion for non-linear triaxial and polyaxial strength of intact rocks. *International Journal of Rock Mechanics and Mining Sciences*, Volume 48, Issue 4, Pages 546-555, ISSN 1365-1609,
5. Muralha, J., Grasselli, G., Tatone, B., et al. (2014). ISRM Suggested Method for Laboratory Determination of the Shear Strength of Rock Joints: Revised Version. *Rock Mech Rock Eng* 47, 291–302. <https://doi.org/10.1007/s00603-013-0519-z>
6. Nassir, M. & Settari, A. & Wan, R. (2013). Joint Stiffness and Deformation Behaviour of Discontinuous Rock. *Journal of Canadian Petroleum Technology*. 49. 10.2118/2009-059.
7. Terzaghi, K., Peck, R. B., & Mesri, G. (1996). *Soil mechanics in engineering practice (3rd ed.)*. John Wiley & Sons. Chapter 4, pages 95-110.